Scientific Research Publishing

Open Journal of Physical Chemistry, 2026, 16(1), 25-38
https://www.scirp.org/journal/ojpc
ISSN Online: 2162-1977
ISSN Print: 2162-1969

Langmuir and Freundlich Isotherms and Pseudo-Order Kinetics of Xylene Adsorption on Succinic Acid-Modified Hardwood Sawdust

Idongesit Effiong Ekpo[1*], Nwamaka Chiagozie Onyemaobi[1], Itoro Esiet Udo[2]

[1]Department of Pure and Industrial Chemistry, Faculty of Science, University of Port Harcourt, Choba, Nigeria
[2]Department of Chemistry, Faculty of Physical Sciences, University of Uyo, Uyo, Nigeria
Email: *idongesit.ekpo@uniport.edu.ng

How to cite this paper: Ekpo, I.E., Onyemaobi, N.C. and Udo, I.E. (2026) Langmuir and Freundlich Isotherms and Pseudo-Order Kinetics of Xylene Adsorption on Succinic Acid-Modified Hardwood Sawdust. *Open Journal of Physical Chemistry*, **16**, 25-38.
https://doi.org/10.4236/ojpc.2026.161002

Received: December 22, 2025
Accepted: February 23, 2026
Published: February 26, 2026

Abstract

In this study, batch sorption of xylene on chemically modified hardwood sawdust (0.1, 0.2, 0.3, 0.4, and 0.5 M) was conducted. Pseudo-first-order (PFO) and pseudo-second-order (PSO) kinetic models were derived from time-dependent uptake data, and isotherms (Langmuir and Freundlich) were also obtained. The linearized Langmuir regression produced an apparent capacity of $Q_m \approx 2.5 \times 10^4$ mg·g^{-1}. However, it yielded a negative physical affinity constant ($K_L < 0$), indicating that the Langmuir assumptions do not apply to this system and that the estimated Q_m should be interpreted as an overall (apparent) sorption capacity rather than a monolayer adsorption capacity. A strong regression was observed in the Freundlich plots. However, the sign of the fitted slope ($1/n$) was non-physical, suggesting that equilibrium was not achieved uniformly across concentrations or that non-ideal mechanisms (e.g., matrix partitioning/capillary retention in a non-single-phase system) contributed to uptake. Kinetically, PSO provided a better description of the uptake curve than PFO under the studied conditions. The enhanced performance of succinic-acid-modified sawdust is attributed to increased accessible sorption domains and strengthened non-specific interactions (hydrophobic and π–π interactions) with aromatic xylene. It was concluded that the modified sawdust is a potential, low-cost lignocellulosic sorbent for aromatic hydrocarbons. It is also necessary to consider the need for equilibrium validation and model selection based on physically meaningful parameters.

Keywords

Xylene Adsorption, Succinic-Acid-Modified Sawdust, Adsorption Capacity, Langmuir Isotherm, Freundlich Isotherm, Pseudo-First-Order Kinetics, Pseudo-Second-Order Kinetics, Chemisorption

1. Introduction

Adsorption is a separation technique in which substances in the gaseous or liquid phase, known as adsorbate, accumulate on the surface of a solid material or the adsorbent. This makes the adsorbate more concentrated at the interface compared to the bulk phase [1]. This process is high in selectivity, efficiency, and versatility, thereby making it widely applicable as a separation technique for removing contaminants or selectively concentrating target substances from mixtures. Absorption involves diffusion of molecules into the bulk of the substrate, while adsorption is restricted to surface interactions. The substrates here are referred to as adsorbents, which are substances with specific surface chemistry, high surface area, and porosity [2]-[4]. Examples of adsorbents are activated carbon, silica gel, alumina, and zeolites [5]. Molecules of the substances usually interact with the adsorbents in one of the following four ways, depending on physicochemical properties of both the adsorbate and adsorbent: surface adsorption of solutes, capillary condensation in pores, ion exchange adsorption, and film formation at interfaces [6]-[9].

The extent of adsorption is typically represented by isotherm models that relate the amount adsorbed to the equilibrium concentration [10]. Two classical models are as follows:

- Langmuir Isotherm: Assumes monolayer adsorption on homogeneous surfaces with finite active sites.
- Freundlich Isotherm: An empirical model describing adsorption on heterogeneous surfaces with multilayer coverage.

These models are crucial for quantifying adsorption capacity and designing large-scale adsorption separation processes [11].

Adsorption isotherm models are generally graphs that enable us to understand the interaction between the volumes of adsorbate extracted from the liquid or gaseous phase and the adsorbent unit mass at constant temperature [12] [13]. This work aims to discover modern adsorbents to boost adsorbent extraction performance and yield an optimal adsorption medium. Adsorption isotherm information can be used to research the quality of an adsorbent. This study considers the use of the Langmuir isotherm, the Freundlich isotherm, pseudo-first-order kinetics, and pseudo-second-order kinetics to determine the potential of a hardwood succinic acid-modified adsorbent for the adsorption of xylene.

2. Experimental Procedure

2.1. Materials and Methods

2.1.1. Sample Preparation

The hardwood sawdust collected from a sawmill industry was prepared and characterized as suitable for pollution remediation [14]. The sawdust was washed with warm water to remove dirt, fungus, and other foreign materials, and then sun-dried for a full day. The sawdust was oven-dried at 110˚C until a constant drying weight was obtained. Afterwards, it was sieved to not more than 0.425 mm. The

modification was performed using the method [15]. 10 g of the dried sample of sawdust was placed in a flat-bottomed flask, soaked, and mixed with 200 ml of a 0.5 M succinic acid solution. The mixture was continuously stirred and refluxed for 4 hours at 75˚C, then cooled to room temperature and filtered using Whatman No. 42 filter paper; the residue was washed with distilled water and dried at 120˚C until a constant drying weight was achieved.

2.1.2. Batch Adsorption of Xylene

The adsorption method used was batch adsorption, similar to that of [16]. The adsorption was carried out at a controlled laboratory temperature of 24˚C - 26˚C. Using a FA/JA-B series analytical balance manufactured by Tianjin Tianma Hengji Instrument Co., Ltd., 0.2 g of sawdust was weighed, then introduced into five 250 ml glass-stoppered conical flasks and placed on the IKA KS 260 Orbital Mechanical Shaker. 100 ml of five different concentrations (0.5, 0.4, 0.3, 0.2, and 0.1 M) xylene and water cosolvent were introduced into glass-stoppered conical flasks. The mechanical shaker was set to agitate at 300 rpm, and the process was run for 15, 30, 60, 90, and 120 min to assess the performance of the adsorption process.

2.1.3. Determination of the Amount of Xylene Adsorbed by the Modified Sawdust

UV/Vis spectrophotometric analysis was carried out to determine the concentration of xylene remaining after batch sorption at 15, 30, 60, 90, and 120 min, using the 1801 UV-VIS Spectrophotometer manufactured by Shanghai Yoke Instrument Co., Ltd. During the study, the filtrates after batch adsorption were collected in cuvettes and placed in a UV/Vis spectrophotometer at wavelengths of 267 - 307 nm. The xylene sample in the cuvette absorbs UV or visible radiation, and the xylene concentration in solution was determined. The amount of light absorbed by the xylene solution depended on the concentration of xylene in the solution, the path length of the cuvette, and how well the xylene absorbed the light at a specific wavelength. Transmittance indicates the concentration of the analyte in the sample [17].

2.2. Adsorption Models

2.2.1. Langmuir Isotherm

The Langmuir isotherm, which was originally designed to describe gas-solid phase adsorption, is also used to evaluate the adsorptive capacity of various adsorbents [18] [19]. It accounts for the surface coverage by balancing the relative rates of adsorption and desorption [20]. It assumes that the rate at which adsorption sites are occupied is proportional to the number of unoccupied sites and that adsorption is limited to a monolayer. Equation (1) represents the Langmuir equation [21]:

$$\frac{C_e}{q_e} = \frac{1}{q_m K_L} + \frac{C_e}{q_m} \tag{1}$$

where:

C_e: Concentration of adsorbate at equilibrium (mg/L).

q_e: Equilibrium monolayer adsorption capacity of the adsorbent (mg/g).

K_L: Langmuir adsorption constant (L/mg) related to the energy of adsorption, which quantitatively reflects the affinity between the adsorbent and the adsorbate.

q_m: Maximum monolayer adsorption capacity of the adsorbent (mg/g).

The linear plot of C_e/q_e as a function of C_e determines the q_m and K_L constants.

The separation factor (R_L) expresses the level of success of the adsorption technique in relation to the model [22] [23]. R_L can be derived from the formula in Equation (2):

$$R_L = \frac{1}{1 + K_L C_o} \tag{2}$$

K_L: Langmuir constant in (mg/L).

C_0: Adsorbate's initial concentration (mg/L).

R_L: Values indicate that adsorption could be unfavourable when $R_L > 1$, linear when $R_L = 1$, favourable when $0 < R_L < 1$, and irreversible when $R_L = 0$.

2.2.2. Freundlich Isotherm

The Freundlich isotherm is suitable for adsorption processes that occur on heterogeneous surfaces [24] [25]. The linear form of the Freundlich isotherm is shown in Equation (3):

$$\ln q_e = \ln K_F + \frac{1}{n} \ln C_e \tag{3}$$

where:

q_e: Adsorption capacity at equilibrium (mg/g);

C_e: The concentration of adsorbate at equilibrium (mg/g);

K_F is the Freundlich constant indicative of adsorption capacity [$(mg \cdot g^{-1})(L \cdot mg^{-1})^{1/n}$];

$1/n$ is the adsorption intensity; it is also indicative of the relative distribution of the energy and defines the heterogeneity of the adsorbate sites [26] [27].

2.2.3. Adsorption Kinetic Models

The kinetics models basically measure the adsorption uptake with respect to time, which further provides useful information concerning the reaction pathways and the mechanism of the sorption reaction [28] [29]. The following are examples of kinetic models: Lagergren pseudo-first order, pseudo-second order, intraparticle diffusion, and liquid film diffusion. In the course of this study, the two kinetic models used were the pseudo-first-order (PFO) and the pseudo-second-order kinetics (PSO). These were compared in this study.

2.2.4. Pseudo-first Order Kinetics

The Lagergren pseudo-first-order kinetic model is commonly applied to describe the rate of solute adsorption onto an adsorbent surface. It assumes that the rate of occupancy of adsorption sites is equal to the number of unoccupied sites. The pseudo-first-order kinetic model is shown in Equation (4):

$$\ln\left(q_e - q_t\right) = \ln\left(q_e\right) - K_1 t \tag{4}$$

where:

q_e = adsorption capacity at equilibrium (mg/g);

q_t = adsorption capacity at time t (min);

t = contact time (min);

K_1 = Lagergren rate constant for pseudo-first-order kinetics.

The plot of $\ln(q_e - q_t)$ as a function of t gives the slope and intercept, which are used to determine the rate constant (K_1) and adsorption capacity (q_e) [30] [31].

2.2.5. Pseudo-Second-Order Kinetics

The formula for pseudo-second-order kinetics is represented in the form proposed by [27], as shown in Equation (5).

The pseudo-second order kinetic model is widely used to describe adsorption processes controlled by surface reaction or adsorption capacity. From the pseudo-second order kinetic model, it can be predicted that the adsorption rate is equal to the square of the number of unoccupied sites. The model is particularly useful in describing adsorption where chemical interactions, such as electron sharing or exchange, dominate.

The linear form of the pseudo-second-order equation is expressed as:

$$\frac{t}{q_t} = \frac{t}{K_2 q_e^2} + \frac{t}{q_e} \tag{5}$$

where:

q_e = adsorption capacity at equilibrium (mg/g);

q_t = adsorption capacity at time t (mg/g);

K_2 = pseudo-second-order rate constant (g/mg·min);

t = contact time (min).

From a plot of (t/q_t) versus t:

Slope = $1/q_e$.

Intercept = $t/\left(k_2 \cdot q_e^2\right)$ was applied for determining their constants.

3. Results and Discussion

3.1. Data Description

3.1.1. Descriptions of the Langmuir Isothermal Model from the Study

The Langmuir linear plots of C_e/q_e versus C_e, showing the removal of xylene from 0.1 - 0.5 M cosolvent solutions using hardwood sawdust modified with 0.5 M succinic acid, are shown in **Figure 1**. The abscissa spans approximately 1900 - 2700 mg/L, and the ordinate ranges from 0.05 to 0.70 g/L. Five series are colour- and marker-coded and listed in the legend (0.5 M, green circles; 0.4 M, blue diamonds; 0.3 M, orange squares; 0.2 M, grey triangles; 0.1 M, yellow crosses). Each series appears as a short linear segment with its least-squares fit equation and coefficient of determination annotated on the plot (R^2 = 0.9997 - 0.9999): $y = 4 \times 10^{-5}x - 0.0047$ (0.5 M), $y = 5 \times 10^{-5}x - 0.007$ (0.4 M), $y = 7 \times 10^{-5}x - 0.0123$ (0.3 M), $y = 1 \times 10^{-4}x - 0.0283$ (0.2 M), and $y = 3 \times 10^{-4}x - 0.1383$ (0.1 M). The vertical place-

ment of the series increases from the 0.5 M data at the lowest C_e/q_e values to the 0.1 M data at the highest. Approximate data spans are as follows: 0.1 M, $C_e \approx$ 2050 - 2410 mg·L^{-1} and $C_e/q_e \approx$ 0.45–0.65 mg·L^{-1}; 0.2 M, $C_e \approx$ 2120 - 2430 mmg·L^{-1} and $C_e/q_e \approx$ 0.22 - 0.27 mg·L^{-1}; 0.3 M, $C_e \approx$ 2210 - 2420 mmg·L^{-1} and $C_e/q_e \approx$ 0.18 - 0.22 mg·L^{-1}; 0.4 M, $C_e \approx$ 2280 - 2490 mmg·L^{-1} and $C_e/q_e \approx$ 0.11 - 0.14 mg·L^{-1}; 0.5 M, $C_e \approx$ 2310 - 2600 mmg·L^{-1} and $C_e/q_e \approx$ 0.09 - 0.11 mg·L^{-1}.

3.1.2. Descriptions of the Freundlich Isothermal Model from the Study

From the 0.1 - 0.5 M xylene cosolvent solution, the Freundlich linear plots in Figure 2 show the removal of the adsorbate from the solution using the 0.5 M

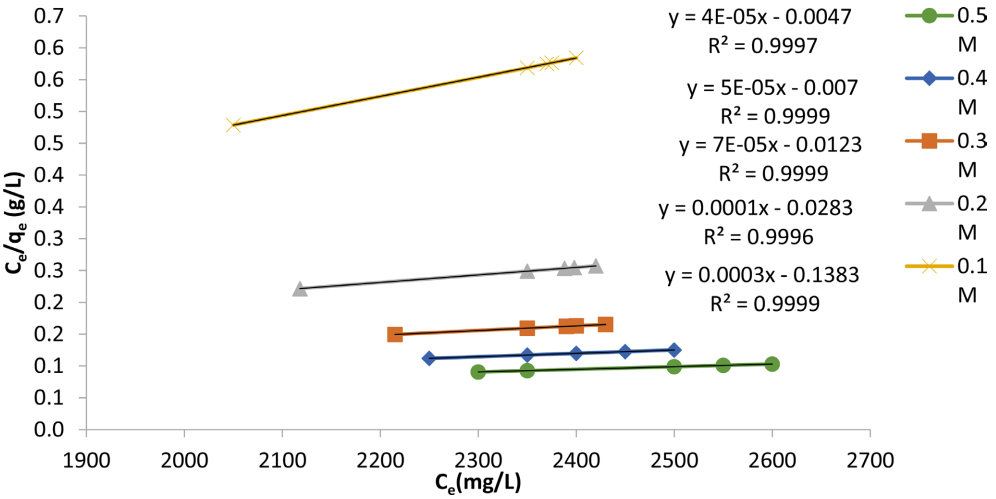

Figure 1. Langmuir isothermal model (C_e/q_e vs. C_e) for xylene removal from 0.1 M, 0.2 M, 0.3 M, 0.4 M, and 0.5 M solutions using 0.5 M succinic acid modified hardwood sawdust as the adsorbent.

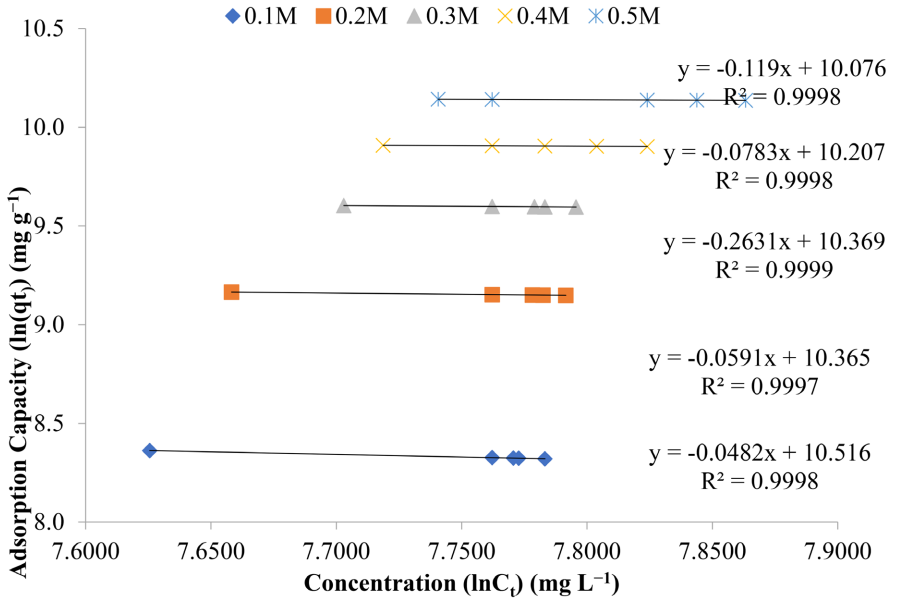

Figure 2. Freundlich isothermal model (logarithmic linear plot) for xylene removal from 0.1 M, 0.2 M, 0.3 M, 0.4 M, and 0.5 M solutions using 0.5 M succinic-acid-modified hardwood sawdust as the adsorbent.

succinic acid modified sawdust; five data series corresponding to five plots display the five initial xylene concentrations, distinguished by different marker shapes and colours (legend row at the top). As shown in the figure, the axes are presented in the logarithmic form used for the Freundlich linearization. The abscissa is 7.00 - 7.35 and the ordinate 9.2 - 10.4. Each series appears as a short, nearly horizontal line segment with a superimposed least-squares fit. On the right-hand side of the plot are the fitted equations, showing small negative slopes with high linearity ($R^2 \approx 0.9997$ - 0.9999); the reported slopes are −0.0482, −0.0591, −0.0783, −0.119, and −0.2631, with intercepts close to 10.xx as displayed. The five clusters are vertically separated, with their data points concentrated within a narrow x-range for each series.

3.1.3. Descriptions of the Lagergren Pseudofirst-Order Kinetics from the Study

The Lagergren pseudo-first-order linear plots of $\ln(q_e - q_t)$ versus time for xylene removal from 0.1 - 0.5 M cosolvent solutions are shown in Figure 3 using 0.5 M succinic-acid-modified hardwood sawdust. The abscissa is time (min), spanning approximately 0 - 140 min, and the ordinate is $\ln(q_e - q_t)$, spanning about 0 - 7. Five data series corresponding to the initial xylene concentrations of 0.1 M, 0.2 M, 0.3 M, 0.4 M, and 0.5 M are distinguished by different markers and colours, with the legend shown on the right of the plot. For each series, four measurement times are plotted (≈20, 40, 60, and 120 min). Least-squares fitted straight lines: 0.1 M, $y = -0.0401x + 6.5937$ ($R^2 = 0.5729$); 0.2 M, $y = -0.0393x + 6.4015$ (R^2 =

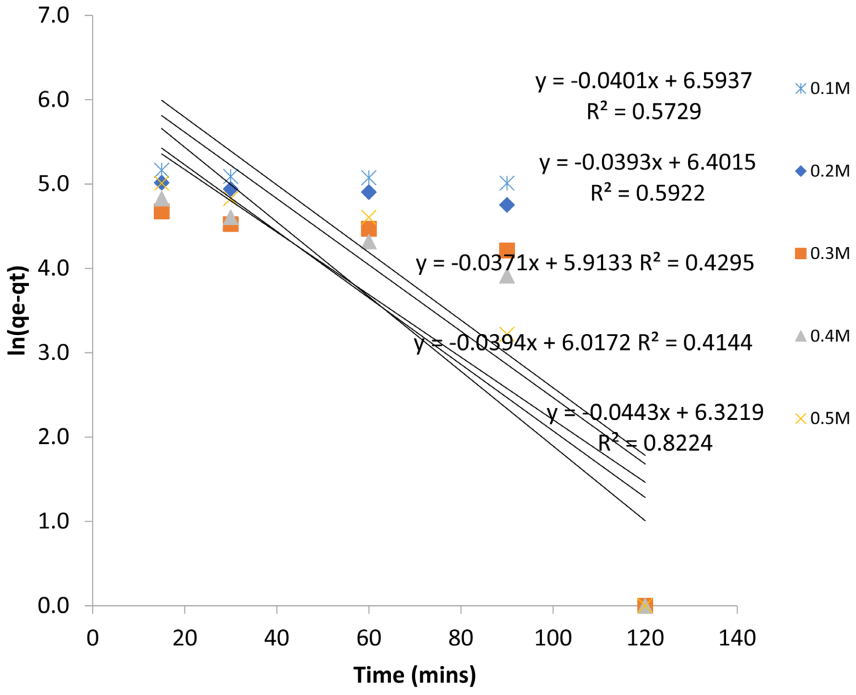

Figure 3. Lagergren pseudo-first-order kinetics ($\ln(q_e - q_t)$ vs. time) for xylene removal from 0.1 M, 0.2 M, 0.3 M, 0.4 M, and 0.5 M solutions using 0.5 M succinic-acid-modified hardwood sawdust as an adsorbent

0.5922); 0.3 M, $y = -0.0371x + 5.9133$ ($R^2 = 0.4295$); 0.4 M, $y = -0.0394x + 6.0172$ ($R^2 = 0.4144$); and 0.5 M, $y = -0.0443x + 6.3219$ ($R^2 = 0.8224$), are overlaid and annotated on the right with their equations and coefficients of determination. The data points at 20 - 60 min cluster in the upper portion of the y-axis (≈4.3 - 5.2), and the 120-min points appear near the lower end of the y-axis, as displayed. Multiple black straight lines are visible across the figure, representing the linear fits.

3.1.4. Descriptions of Pseudosecond-Order Kinetics from the Study

Similarly, the pseudo-second-order linear plots (t/q_t versus time) for xylene removal from 0.1–0.5 M cosolvent solutions using hardwood sawdust modified with 0.5 M succinic acid as the adsorbent are shown in **Figure 4**. The abscissa is time (min), extending from 0 to approximately 140 min, and the ordinate is t/q_t, ranging from about 0.0000 to 0.0300. Five data series, with one for each initial concentration (0.1 M, 0.2 M, 0.3 M, 0.4 M, and 0.5 M), are distinguished by different marker shapes and colours as indicated in the legend at the right. For each series, four measurement times are shown (≈20, 40, 60, and 120 min). For each xylene concentration, the equations and coefficients of determination are shown on the straight line least squares fits that are superimposed in black as follows: 0.1 M, $y = 0.0002x + 0.0003$ ($R^2 = 0.9991$); 0.2 M, $y = 0.0001x + 5E{-}05$ ($R^2 = 0.9999$); 0.3 M, $y = 7E{-}05x + 2E{-}05$ ($R^2 = 0.9999$); 0.4 M, $y = 5E{-}05x + 9E{-}06$ ($R^2 = 0.9999$); and 0.5 M, $y = 4E{-}05x + 7E{-}06$ ($R^2 = 0.9999$). The data points for each concentration align closely with their respective fitted lines within a narrow x-range at each time point.

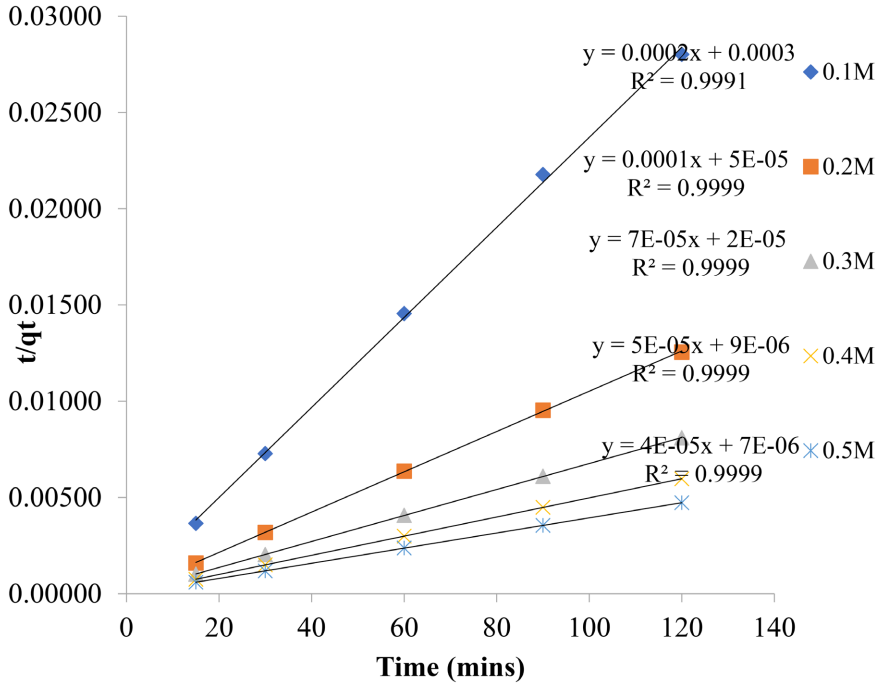

Figure 4. Pseudo-second-order kinetics (t/q_t vs. time) for xylene removal from 0.1 M, 0.2 M, 0.3 M, 0.4 M, and 0.5 M solutions using 0.5 M succinic-acid-modified hardwood sawdust as the adsorbent.

3.2. Deductions from Data

3.2.1. Deductions from the Langmuir Isothermal Model in the Study

Figure 1 shows the linearized Langmuir relationships for the investigated xylene concentration levels, and the corresponding regression and derived parameters are summarized in Table 1. Although the regressions exhibit near-unity linearity, the intercepts are consistently negative, which forces negative K_L values and consequently negative R_L values; this outcome is non-physical within the Langmuir framework and indicates that the Langmuir model assumptions are not satisfied for the present system. The derived Q_m values should therefore be interpreted only as *apparent* capacities from the linearization rather than true monolayer capacities. Non-Langmuir behaviour is traceable to the very high apparent uptake; this reflects heterogeneous sorption domains as well as contributions from non-ideal mechanisms (matrix partitioning and capillary retention). It may also be because the capacity approached the mass balance limit at the highest initial concentration [11] [21] [32] [33].

3.2.2. Deductions from the Freundlich Isothermal Model from the Study

Figure 2 presents the Freundlich-type linear regressions for xylene uptake on succinic-acid-modified sawdust, and the corresponding regression and derived parameters are summarized in Table 2. For the dataset described by the trendline, the negative slope implies a non-physical process and is not typical for an adsorption isotherm, because it would correspond to a decrease in q_e with increasing C_e. Also, the R-square value near unity is not considered a validation of the Freundlich applicability, but rather an indication that linearization fits a narrow data band and yields parameters that are not physically interpretable under the Freundlich models.

Table 1. Langmuir Isotherm parameters.

Xylene solution (M)	Slope	Intercept	Q_m (mg/g)	K_L (L/mg)	R_L
0.1	0.0003	−0.1383	3333	−0.002169	−0.0454
0.2	0.0001	−0.0283	10,000	−0.003534	−0.01351
0.3	0.00007	−0.0123	14,286	−0.005691	−0.005548
0.4	0.00005	−0.0070	20,000	−0.007143	−0.003308
0.5	0.00004	−0.0047	25,000	−0.008511	−0.002219

Table 2. Freundlich isotherm parameters.

Xylene solution (M)	Trendline Slope = $1/n$	n = 1/slope	R^2
0.1	−0.0482	−20.747	0.9998
0.2	−0.0591	−16.920	0.9997
0.3	−0.2631	−3.801	0.9999
0.4	−0.783	−12.771	0.9998
0.5	−0.1190	−8.403	0.9998

A negative $1/n$ commonly indicates that the points used in the fit do not represent a consistent equilibrium state and/or that non-ideal effects are influencing the calculated q_e values. Possible reasons for the process not aligning with true equilibrium typical of surface adsorption are: the inability of the dataset used for regression to attain equilibrium; distortion in mass balance; and non-single-phase behaviour of xylene in water. These signify more of sorption processes, such as partitioning into the lignocellulosic matrix and pore filling. The intercept (10.1) corresponds to $\ln K_F$ in the natural-log form, giving an apparent $K_F \approx e^{10.1} \approx 2.4 \times 10^4$, but because $1/n$ is negative, this K_F value is an empirical outcome of the regression, not a reliable measure of adsorption capacity or favourability. Successes in removing xylene in the study could be attributed to non-specific interactions, such as hydrophobic and π-π interactions.

3.2.3. Deductions from Lagergren Pseudofirst-Order Kinetics from the Study

Figure 3 shows the pseudo-first-order kinetic plots for xylene at different concentrations with 0.5 M succinic acid-modified sawdust. For 0.5 M xylene concentration (orange square symbols):

$$\text{Equation: } y = -0.0443x + 6.3219 \text{ with } R^2 = 0.8224$$

From the equation, the slope, intercept, and R^2 values are shown as $-0.0443 = -k_1 \rightarrow k_1 = 0.0443\ \text{min}^{-1}$, $6.3219 = \ln(q_e) \rightarrow q_e = \exp(6.3219) \approx 555$ mg/g, and 0.8224, respectively. The slope represents the pseudo-first-order rate constant, which indicates a moderate adsorption rate for xylene onto 0.5 M succinic acid–modified sawdust. The equilibrium adsorption capacity $q_e \approx 555$ mg/g demonstrates a high capacity for xylene removal.

The R^2 value indicates a fair correlation with the pseudo-first-order kinetic model, suggesting that the adsorption process may not be purely first-order and that other kinetic models (e.g., pseudo-second-order) could provide a better fit.

The kinetic analysis confirms that the adsorption of xylene onto 0.5 M succinic acid–modified sawdust occurs at a measurable rate that depends on the availability of active sites.

The modified sawdust shows significant potential for practical application, given its high q_e value and reasonable kinetic performance.

The deviation from perfect linearity ($R^2 < 0.9$) implies that multiple mechanisms, such as film diffusion and intra-particle diffusion, may influence the adsorption process.

3.2.4. Deductions from Pseudosecond-Order Kinetics in the Study

Figure 4 shows pseudo-second-order kinetic plots for succinic acid-modified sawdust at different concentrations. For the 0.5 M xylene concentration, which is indicated with light blue × symbols:

Equation: $y = 4\text{E}{-}05x + 7\text{E}{-}06$ with $R^2 = 0.9999$, showing a perfect fit to the model.

From the equation:

$$\text{Slope} = 1/q_e \rightarrow q_e = 1/(4 \times 10^{-5}) = 25{,}000 \text{ mg/g}$$

$$\text{Intercept} = 1/\left(k_2 \cdot q_e^2\right)$$

Substituting $q_e = 25{,}000$ mg/g:

$$k_2 = 1/(\text{intercept} \times q_e^2)$$

$$k_2 = 1/(7 \times 10^{-6} \times (25{,}000^2))$$

$$k_2 \approx 2.29 \times 10^{-4} \text{ g/mg·min}$$

The near-excellent fit R-square of 0.9991-0.9999 for the pseudo-second order model confirms that chemisorption is the dominant mechanism for xylene adsorption onto 0.5 M succinic acid-modified sawdust. It also validates pseudo-second-order kinetics as the most accurate descriptor for this adsorption system, compared to pseudo-first-order behaviour.

An efficient adsorption kinetics is indicated by the moderate rate constant k_2, which balances high uptake with steady reaction rates.

Succinic acid modification introduces carboxyl groups that strongly interact with aromatic xylene molecules, supporting a chemisorption-controlled process.

The high q_t value highlights the potential of 0.5 M modified sawdust for practical water treatment applications, where high pollutant removal efficiency is essential.

4. Conclusions

Hardwood sawdust modified with succinic acid proved to be a cost-effective adsorbent for the removal of xylene from aqueous solution. Langmuir linearization of the equilibrium data over the investigated xylene concentration range (0.1 - 0.5 M) produced an excellent regression (reported $R^2 \approx 0.9996$ - 0.9999) and an apparent maximum capacity of $Q_m \approx 2.5 \times 10^4$ mg g^{-1}. However, the Langmuir parameters are best interpreted as empirical descriptors rather than definitive evidence of monolayer adsorption.

Freundlich linearization also yielded near-unity regression ($R^2 \approx 0.9997$ - 0.9999) and indicated a comparatively large K_F, consistent with strong overall sorption and the presence of heterogeneous sorption domains. Under the standard Freundlich sign convention, values of $n > 1$ indicate favorable sorption. Overall, the equilibrium behaviour is more consistent with heterogeneous and non-ideal uptake mechanisms than with strict Langmuir monolayer coverage, and kinetic analysis showed the pseudo-first-order model, which described the data fairly well for 0.5 M adsorption. However, the pseudo-second-order model yielded near-unity linearity over all concentrations, supporting a rate controlled primarily by site occupancy on the modified surface.

Overall, the data indicated rapid uptake followed by a high-capacity monolayer on a heterogeneously functionalized surface, plausibly mediated by carboxyl-driven interactions (π-π and hydrophobic effects). Given the combination of very high capacity and moderate affinity, 0.5 M succinic acid modification of sawdust is a promising route for polishing xylene-bearing wastewaters and related BTEX streams.

Acknowledgements

The authors are thankful to the Department of Pure and Industrial Chemistry, University of Port Harcourt, and Ideal Geo-chem and Environmental Services Limited for providing the instruments and reagents that were used in carrying out this study.

Conflicts of Interest

The authors declare no conflicts of interest regarding the publication of this paper.

References

[1] Ruthven, D.M. (1984) Principles of Adsorption and Adsorption Processes. Wiley.

[2] Wang, J. and Guo, X. (2020) Adsorption Isotherm Models: Classification, Physical Meaning, Application and Solving Method. *Chemosphere*, **258**, Article 127279. https://doi.org/10.1016/j.chemosphere.2020.127279

[3] IUPAC (2025) Adsorption. In: *IUPAC*: *Compendium of Chemical Terminology* (5th ed., Online Version 5.0.0), International Union of Pure and Applied Chemistry, Orange Book, 2nd ed., p. 85.

[4] Adsorption (2025) Wikipedia. https://en.wikipedia.org/wiki/Adsorption?utm

[5] Yang, R.T. (2003) Adsorbents: Fundamentals and Applications. Wiley.

[6] Rouquerol, J., Rouquerol, F., Llewellyn, P., Maurin, G. and Sing, K.S.W. (2014) Adsorption by Powders and Porous Solids: Principles, Methodology and Applications. 2nd Edition, Academic Press.

[7] Sivakumar, D., Nouri, J., Modhini, T.M. and Deepalakshmi, K. (2018) Nickel Removal from Electroplating Industry Wastewater: A Bamboo Activated Carbon. *Global Journal of Environmental Science and Management*, **4**, 325-338.

[8] Gregg, S.J. and Sing, K.S.W. (1982) Adsorption, Surface Area and Porosity. 2nd Edition, Academic Press.

[9] Crittenden, J.C., Trussell, R.R., Hand, D.W., Howe, K.J. and Tchobanoglous, G. (2012) MWH's Water Treatment: Principles and Design. 3rd Edition, Wiley.

[10] Alan-Gabelman, P.E. (2017) Absorption Basics: Part 1. American Institute of Chemical Engineers. Gabelman Process Solutions, LLC.

[11] Foo, K.Y. and Hameed, B.H. (2010) Insights into the Modeling of Adsorption Isotherm Systems. *Chemical Engineering Journal*, **156**, 2-10. https://doi.org/10.1016/j.cej.2009.09.013

[12] Vaghetti, J.C.P., Lima, E.C., Royer, B., Brasil, J.L., da Cunha, B.M., Simon, N.M., *et al.* (2008) Application of Brazilian-Pine Fruit Coat as a Biosorbent to Removal of Cr(VI) from Aqueous Solution—Kinetics and Equilibrium Study. *Biochemical Engineering Journal*, **42**, 67-76. https://doi.org/10.1016/j.bej.2008.05.021

[13] Zhou, Y., Ge, L., Fan, N. and Xia, M. (2012) Adsorption of Congo Red from Aqueous Solution onto Shrimp Shell Powder. *Adsorption Science & Technology*, **36**, 1310-1330. https://doi.org/10.1177/0263617418768945

[14] Nwufo, B.T., Isaac, N.D. and Onche, E.U. (2014) Preparation and Characterization of Sawdust (Cellulose) as an Adsorbent for Oil Pollution Remediation. *International Journal of Natural Sciences Research*, **2**, 97-102.

[15] Mutiara, T., Karisa, P.C. and Mujahidah, I. (2018) Acid Modified Jackfruit Wood

Sawdust as Biosorbent for the Removal of Fe(II) from Aqueous Solutions. *MATEC Web of Conferences*, **154**, Article 1019. https://doi.org/10.1051/matecconf/201815401019

[16] Nordine, N., El Bahri, Z., Sehil, H., Fertout, R.I., Rais, Z. and Bengharez, Z. (2016) Lead Removal Kinetics from Synthetic Effluents Using Algerian Pine, Beech and Fir Sawdust's: Optimization and Adsorption Mechanism. *Applied Water Science*, **6**, 349-358. https://doi.org/10.1007/s13201-014-0233-3

[17] Hooijschuur, J.H. (2025) UV/Vis Spectrometry Basics. Chromedia. https://www.chromedia.org/chromedia?waxtrapp=lnijabEsHiemBpdmBlIEcCJlBN

[18] Langmuir, I. (1918) The Adsorption of Gases on Plane Surfaces of Glass, Mica and Platinum. *Journal of the American Chemical Society*, **40**, 1361-1403. https://doi.org/10.1021/ja02242a004

[19] Elmorsi, T.M. (2011) Equilibrium Isotherms and Kinetic Studies of Removal of Methylene Blue Dye by Adsorption onto Miswak Leaves as a Natural Adsorbent. *Journal of Environmental Protection*, **2**, 817-827. https://doi.org/10.4236/jep.2011.26093

[20] Günay, A., Arslankaya, E. and Tosun, İ. (2007) Lead Removal from Aqueous Solution by Natural and Pretreated Clinoptilolite: Adsorption Equilibrium and Kinetics. *Journal of Hazardous Materials*, **146**, 362-371. https://doi.org/10.1016/j.jhazmat.2006.12.034

[21] Dąbrowski, A. (2001) Adsorption—From Theory to Practice. *Advances in Colloid and Interface Science*, **93**, 135-224. https://doi.org/10.1016/s0001-8686(00)00082-8

[22] Hart, P.J., Vastola, F. and Walker Jr, P.L. (1987) Oxygen Chemisorptions on Well Cleaned Carbon Surfaces. *Carbon*, **5**, 363-371.

[23] Dike, O.E. (2019) M-Xylene Removal from Aqueous Solution Using Organic Acid Modified Bentonite: Effect of Dissociation Constant of the Organic Acids.

[24] Freundlich, H. (1907) Über die Adsorption in Lösungen. *Zeitschrift für Physikalische Chemie*, **57**, 385-470. https://doi.org/10.1515/zpch-1907-5723

[25] Ayawei, N., Angaye, S.S., Wankasi, D. and Dikio, E.D. (2015) Synthesis, Characterization and Application of Mg/Al Layered Double Hydroxide for the Degradation of Congo Red in Aqueous Solution. *Open Journal of Physical Chemistry*, **5**, 56-70. https://doi.org/10.4236/ojpc.2015.53007

[26] Boparai, H.K., Joseph, M. and O'Carroll, D.M. (2011) Kinetics and Thermodynamics of Cadmium Ions Removal by Nano Zerovalent Iron: Surface Analysis, Effects of Solution Chemistry and Surface Complexation Modeling. *Environmental Science Pollution Research*, **2**, 6210-6221.

[27] Rao, R.A.K. and Kashifuddin, M. (2014) Kinetics and Isotherm Studies of Cd(II) Adsorption from Aqueous Solution Utilizing Seeds of Bottlebrush Plant (*Callistemon chisholmii*). *Applied Water Science*, **4**, 371-383. https://doi.org/10.1007/s13201-014-0153-2

[28] Ho, Y. and Mckay, G. (2000) The Kinetics of Sorption of Divalent Metal Ions Onto Sphagnum Moss Peat. *Water Research*, **34**, 735-742. https://doi.org/10.1016/s0043-1354(99)00232-8

[29] Hansda, A., Kumar, V. and Anshumali (2015) Biosorption of Copper by Bacterial Adsorbents: A Review. *Research Journal of Environmental Toxicology*, **9**, 45-58. https://doi.org/10.3923/rjet.2015.45.58

[30] Dawodu, F.A. and Akpomie, K.G. (2014) Simultaneous Adsorption of Ni(II) and Mn(II) Ions from Aqueous Solution unto a Nigerian Kaolinite Clay. *Journal of Materials Research and Technology*, **3**, 129-141.

https://doi.org/10.1016/j.jmrt.2014.03.002

[31] Revellame, E.D., Fortela, D.L., Sharp, W., Hernandez, R. and Zappi, M.E. (2020) Adsorption Kinetic Modeling Using Pseudo-First Order and Pseudo-Second Order Rate Laws: A Review. *Cleaner Engineering and Technology*, **1**, Article 100032. https://doi.org/10.1016/j.clet.2020.100032

[32] Ayawei, N., Ebelegi, A.N. and Wankasi, D. (2017) Modelling and Interpretation of Adsorption Isotherms. *Journal of Chemistry*, **2017**, 1-11. https://doi.org/10.1155/2017/3039817

[33] Limousin, G., Gaudet, J.P., Charlet, L., Szenknect, S., Barthès, V. and Krimissa, M. (2007) Sorption Isotherms: A Review on Physical Bases, Modeling and Measurement. *Applied Geochemistry*, **22**, 249-275. https://doi.org/10.1016/j.apgeochem.2006.09.010